ICES Journal of Marine Science
January 2019, Volume 76, Issue 1, Pages 232-243
https://doi.org/10.1093/icesjms/fsy163
https://archimer.ifremer.fr/doc/00468/57967/

Directional bilateral asymmetry in otolith morphology may affect fish stock discrimination based on otolith shape analysis

Mahé Kélig [1, *], Ider Djamila [2], Massaro Andrea [3], Hamed Oussama [4], Jurado-Ruzafa Alba [5], Goncalves Patricia [6], Anastasopoulou Aiketerini [7], Jadaud Angelique [8], Mytilineou Chryssi [7], Elleboode Romain [1], Ramdane Zohir [2], Bacha Mahmoud [9], Amara Rachid [9], De Pontual Hélène [10], Ernande Bruno [1]

[1] Fisheries Laboratory, IFREMER, 150 Quai Gambetta, BP 699, 62 321 Boulogne-sur-Mer, France
[2] Laboratoire de Zoologie Applique´e et d'Ecophysiologie Animale, Universite´ Abderrahmane Mira, Be´jaý¨a, Alge´rie
[3] APLYSIA – Via Menichetti 35, 27121 Livorno, Italy
[4] Universite´ de Tunis El Manar, Campus Universitaire, 2092 El Manar II, Tunisie
[5] Instituto Espa~nol de Oceanografý´a, Centro Oceanogra´fico de Canarias, 38180 Santa Cruz de Tenerife, Spain
[6] Departamento do Mar e Recursos Marinhos, Intituto Portugueˆs do Mar e da Atmosfera (IPMA), Lisboa, Portugal
[7] Hellenic Centre for Marine Research, PO Box 712, P.C. 19013, Anavyssos Attiki, Athens, Greece
[8] Fisheries Laboratory, IFREMER-UMR MARBEC, Avenue Jean Monnet, CS 30171, 34203 Se`te Cedex, France
[9] Laboratoire d'Oce´anologie et de Ge´osciences, Universite´ Littoral Coˆte d'Opale, Univ. Lille, CNRS, UMR 8187, LOG, F 62930 Wimereux, France
[10] IFREMER, Sciences et Technologies Halieutiques, CS 10070, 29280 Plouzane´, France

* Corresponding author : Kélig Mahé, email address : kelig.mahe@ifremer.fr.

Abstract :

Otolith shape analysis is an efficient fish stock identification tool. However, most applications used left and right otoliths or only one of them arbitrarily chosen without testing for biases resulting from potential directional bilateral asymmetry (DA) in otolith shape, i.e. a unimodal population-level deviation form bilateral symmetry between right and left otolith shapes. In this study, 560 bogues (Boops boops) were sampled from 11 geographical locations from the Canary Islands to the Aegean Sea and elliptical Fourier descriptors were used to describe their otoliths' shape. First, a significant otolith DA was observed at the global scale with an average amplitude of 2.77%. However, at the scale of sampling locations, DA was not always significant and varied in amplitude and direction. Second, population structure was investigated using the shape of either right otoliths or left otoliths or both together. Analyses based on right otoliths or both otoliths together, suggested three stock units: a North-Western Mediterranean Sea stock, an Eastern Mediterranean Sea stock, and a Central-Eastern Atlantic Ocean and South-Western Mediterranean Sea stock. In contrast, no coherent geographical pattern was found based on left otoliths. Our results highlight the importance of accounting for potential otolith DA in otolith shape-based stock identification.

Keywords : Boops boops, elliptical Fourier analysis, Mediterranean Sea, side effect, stock identification.

Introduction

Stock identification and the knowledge of population spatial structure provide a basis for understanding fish population dynamics and achieving reliable assessments for fishery management (Reiss *et al.*, 2009). Some studies suggested that a lack of knowledge of population spatial structure in fisheries management might be responsible for fishery collapses (e.g. Atlantic cod (*Gadus morhua*) in the Western Atlantic, Hutchings, 2005; the crustacean fisheries of Alaska, Wooster, 1992; North-Western Atlantic herring, Stephenson *et al.*, 1999). Therefore, a wide number of techniques were developed and applied to identify and discriminate stock units, such as tagging experiments or analyses of spatial variation in arrange of markers including genetic markers, morphological traits, life-history traits at various life-stages, parasite load or infracommunity structure, or contaminant concentration (e.g. Pawson and Jennings, 1996; Garcia *et al.*, 2011; Cadrin *et al.*, 2014; ICES, 2016, Pita *et al.*, 2016). Otoliths are calcified structures overlying the sensory epithelia in the inner ears. The left and right inner ear contain three pairs of otoliths each. They grow throughout the life of the fish and, unlike scales and bones, are metabolically inert (i.e. once deposited, otolith material is unlikely to be resorbed or altered, Casselman, 1987). Consequently, otolith shape remains unaffected by short-

term changes in fish condition (Campana and Casselman, 1993) or environmental variations (Campana, 1999). Shape analysis was first used to discriminate fish stocks by using either scales of Atlantic salmon (*Salmo salar*) (de Pontual and Prouzet, 1987, 1988) or otolith of Atlantic cod (Campana and Casselman 1993). Since then, many studies have focused on otolith-shape analysis to discriminate between stock units, reaching an updated total of 91 papers published from 1993 to 2017 exclusively on this topic.

The shape of a fish's otolith depends on its genotype, its developmental stage (potentially described by a series of individual-state variables such as body size, age, sex and sexual maturity status) and both the biotic and abiotic environments encountered during its lifetime (Castonguay *et al.*, 1991, Lombarte and Lleonart, 1993; Cadrin and Friedland, 1999; Begg and Brown, 2000; Cardinale *et al.*, 2004; Gagliano and McCormick, 2004; Monteiro *et al.*, 2005; Swan *et al.*, 2006; Mérigot *et al.*, 2007; Hüssy, 2008; Vignon and Morat, 2010; Capoccioni *et al.*, 2011; Mille *et al.*, 2016). Besides inter-individual variation, otolith shape is also known to vary potentially intra-individually as left otolith shape may not be perfectly symmetrical to right otolith shape one and vice-versa (Díaz-Gill *et al.*, 2015). Such deviation or bilateral asymmetry can be of three different types corresponding to three different distributions of its individual values within a population (Palmer and Strobeck 1986, 1992). Fluctuating asymmetry (FA) corresponds to random individual deviations from perfect bilateral symmetry resulting in a normal distribution with mean 0. FA in otolith shape has been reported for some species of both roundfish and flatfish (Lemberget and McCormick, 2009; Lychakov, 2013; Díaz-Gil *et al.*, 2015). Directional asymmetry (DA) relates to a systematic deviation from bilateral symmetry towards one side (e.g. the otolith asymmetry in flatfish, Mille *et al.*, 2015) and is thus characterized by a normal distribution with a mean different from 0 whose sign depends on the side of the deviation. Antisymmetry (A) occurs when there is a systematic but alternating deviation towards one side or the other in the population, thus generating a

bimodal distribution with mean 0 in its extreme form (e.g. of the claws of fiddler crabs Palmer and Strobeck,1986; or lobsters Govind and Pearce, 1986). If DA or A occurs, it may affect the results of otolith-shape based stock discrimination, depending on which otolith is used. Among the 91 published studies on marine fish stock identification based on otolith shape analysis, only 20 of them took into account otolith shape asymmetry (A) and only 3 based their analyses on the two otoliths together. Most studies arbitrarily used otoliths from only one side. In this context, the first objective of the present study was to explore the effect of DA in otolith morphology on stock identification based on otolith shape analysis.

To describe the external contour or shape of otoliths, several techniques have been developed: univariate descriptors such as shape factors that include roundness or circularity (e.g.Tuset *et al.*, 2003), geometric morphometrics (e.g. Ponton, 2006; Ramirez-Perez *et al.*, 2010; Vergara-Solana *et al.*, 2013), wavelet functions (Parisi-Baradad *et al.*, 2005; Sadighzadeh *et al.*, 2014), growth markers (Benzinou *et al.*, 2013), curvature scale space (Mapp *et al.*, 2013) and geodesic methods (Benzinou *et al.*, 2013). However, the Elliptical Fourier Analysis (EFA) remains the most widely used method to describe otolith shape. In recent years, the number of studies using EFA has increased substantially and allowed the analysis of population structure of as diverse species as highly migratory oceanic swordfish (*Xiphias gladius*, Mahé *et al.*, 2016) and sedentary big-scale sand smelt (*Atherina boyeri*; Boudinar *et al.*, 2015).

In this paper, we used the bogue (*Boops boops;* Linnaeus, 1758), a species within the Sparidae family, as a case study for assessing the effect of DA and/or A on stock identification based on otolith shape analysis using EFA. This species has a wide geographical distribution from the Norwegian to Angolan coasts along the northeastern Atlantic, as well as in the Mediterranean and Black seas (Whitehead *et al.,* 1984). Bogue is both demersal and semi-pelagic and inhabits all types of seabed (sand, mud, rock and seagrass beds) down to 350m depth, but is most abundant in the upper 100m. It is an

129 important species for Mediterranean fisheries with an average landing of 27,000 tons
130 from 2010 to 2013 (ranked 7th and accounting for 1.8% of total catches in the
131 Mediterranean Sea, FAO, 2016). This species is currently fully exploited by several
132 commercial fisheries, either as a target species or as bycatch, mainly from pelagic
133 trawlers (FAO, 2016; Dimarchopoulou *et al.*, 2017). Moreover, although bogue is one of
134 the seven most studied species in the Mediterranean Sea (Dimarchopoulou *et al.*, 2017),
135 no information is available on its general stock structure. Hence, the second objective of
136 this study was to investigate the stock structure of the bogue in the Mediterranean Sea
137 and the adjacent area of the Atlantic Ocean.

138 To reach the two objectives of this study, i.e. (1) to explore the impact of otolith DA on
139 otolith-shape based stock identification and (2) to investigate bogue stock structure in
140 the Mediterranean Sea, we extract left and right otolith shape using Ellipitical Fourrier
141 descriptors and use them to, first, test for otolith DA and investigate how its varies across
142 sampling locations and, second, investigate stock structure through a combination of
143 linear discriminant analysis and clustering using sequentially the shape of left otoliths
144 only, rights otoliths only and both together.

145

146 ***MATERIALS AND METHODS***

147 ***Sample collection***

148 Sagittal otoliths (left and right) were extracted from a total of 560 individuals ranging from
149 13 to 26 cm total length (mean±SE: 18.38±2.63 cm), collected from 11 locations from the
150 Canary Islands to the Aegean Sea (Figure 1 and Table 1). Samples were collected
151 between 2013 and 2016 by six Institutes (Institut Français de Recherche pour
152 l'Exploitation de la Mer - IFREMER, France; University Abderrahmane Mira, Algeria;
153 APLYSIA institute, Italy; University of Tunis, Tunisia; Instituto Español de Oceanografía
154 - IEO, Spain; Hellenic Centre for Marine Research-HCMR, Greece) during the
155 international bottom trawl survey in the Mediterranean Sea (MEDITS surveys), on board

156 fishing vessels and from fish markets. The sex of the sampled individuals was
157 determined by macroscopic examination of their gonads and only mature fish were
158 included in this study to minimize the effect of sexual maturity, which may affect otolith
159 shape (Cardinale *et al.*, 2004). Moreover, to limit the effect of age on the otolith shape,
160 the age range of fish sampled was limited from two to four years. In order to estimate the
161 age of each individual, whole sagittal otoliths were examined, after cleaning, by two
162 expert age readers in order to limit interpretation errors. To increase the visibility of the
163 growth marks, otoliths were covered with clove essential oil and observed with a
164 stereomicroscope under reflected light on a dark background.

165 ***Otolith shape analysis***

166 A calibrated high-resolution image (3.200 dpi) of the proximal face of the whole left and
167 right sagittal otolith was obtained using a scanner with reflected light (Epson V750).
168 During this process, a fixed single magnification was used to ensure as high a resolution
169 as possible. Image processing was performed using the image analysis system TNPC
170 (Digital processing for calcified structures, version 7) with the *sulcus acusticus* facing up.
171 In order to compare left and right otolith shapes, mirror images of left otoliths were used.
172 The length and width of otoliths were automatically extracted as the largest distance
173 along the antero-posterior axis and the ventro-dorsal axis, respectively.

174 To describe otolith contours, Elliptic Fourier Analysis (e.g. Lestrel, 2008) was carried out
175 on each otolith contour delineated and extracted after image binarization. All Elliptic
176 Fourier Descriptors (EFD's) were obtained by using TNPC 7 software. For each otolith,
177 the first 99 elliptical Fourier harmonics (H) were extracted and normalised with respect
178 to the first harmonic and were thus invariant to otolith size, rotation and starting point of
179 contour description (Kuhl and Giardina, 1982). To determine the number of harmonics
180 required to reconstruct the otolith outline, the cumulated Fourier Power (F) was
181 calculated for each individual otolith as a measure of the precision of contour
182 reconstruction obtained with n_k harmonics (i.e., the proportion of variance in contour
183 coordinates accounted for by the n_k harmonics):

184 $$F_{(n_k)} = \sum_{i=1}^{n_k} \frac{{A_i}^2+{B_i}^2+{C_i}^2+{D_i}^2}{2}$$

185 where A_i, B_i, C_i and D_i are the coefficients of the $H_i$harmonic. $F(n_k)$F and n_k were
186 calculated for each individual otolith k in order to ensure that each individual otolith in
187 the sample was reconstructed with a precision of 99.99% (Lestrel, 2008). The maximum
188 number of harmonics $n = \max(n_k)$ across all otoliths was then used to reconstruct each
189 individual otolith.

190 ***Statistical analyses***

191 DA in otolith shape was analysed as the effect of otolith's location side, i.e., left *versus*
192 right inner ear (side SI, thereafter) on otolith shape. Firstly, Principal Components
193 Analysis (PCA) was applied to the selected Elliptical Fourier Descriptors (EFD's) matrix
194 (*EFD*'s as columns and individual otolith as lines) of otolith contours (Rohlf and Archie,
195 1984) and a subset of the resulting Principal Components (PC's) was selected as otolith
196 shape descriptor according to the broken stick model (Legendre and Legendre, 1998).
197 The matrix of selected PCs, with PCs as columns and otoliths as lines, is referred to as
198 the shape matrix S hereafter. This procedure allowed us to decrease the number of
199 variables used to describe otolith shape variability while ensuring that the main sources
200 of shape variation were accounted for, as well as to avoid co-linearity between shape
201 descriptors (Rohlf and Archie, 1984).

202 The shape matrix (S) was analyzed using the following multivariate mixed-effects model:

203 $$S \sim L + SI + LO + SI{:}\,LO + i$$

204 where otolith shape variations due to side (SI), sampling location (LO) and their
205 interaction ($SI{:}\,LO$) are represented by fixed effects. More precisely, SI measures DA at
206 the global scale, LO assesses shape variation across sampling locations affecting both
207 otoliths and $SI{:}\,LO$ represents variation in DA across sampling locations. Individuals' total
208 length L was also included as a covariate to remove some potentially confounding

ontogenetic effect on otolith shape. Finally, a random intercept (i) was used to account for variability due to individuals (or some of their characteristics, such as total length for instance) and autocorrelation between left and right otolith shape within individuals. The model was fitted with a different variance for each PC of the shape matrix S. Normality of the residuals and the random effects as well as homoscedasticity of the residuals were assessed by visual inspection of diagnostic plots. The significance of explanatory variables at 5% was tested by likelihood ratio tests between nested models while respecting marginality of the effects (type 2 tests; Fox and Weisberg 2011) that are supposed to follow a χ^2 distribution under the null hypothesis. To visualise differences in otolith shape between right and left sides, an average otolith shape was rebuilt for each side based on EFD's. Moreover, the direction and amplitude of DA at the global scale and at each sampling location was extracted from the multivariate mixed-effects model as the estimators of the side effect SI and of the interaction between head side and sampling location $SI{:}LO$, respectively. To ease interpretation, it was also evaluated as the average percentage of non-overlapping surface between the right and left otoliths' shapes reconstructed on the basis of the EFD's at the individual level. The percentage was computed relative to the total area.

To discriminate fish from the 11 sampled locations based on otolith shape, a Linear Discriminant Analysis (LDA) with jacknifed prediction was applied to the residuals R_S of a redundancy analysis (RDA) $S{\sim}L$ of the shape matrix S explained by individuals' total length L. The use of the residual matrix R_S instead of the shape matrix S was meant to avoid potential confounding effects due to otolith shape variation across sampling locations related to variations in individuals' size originating from different size-selectivity of the capture procedure/gear at different sampling sites (Rencher and Christensen, 2012). To evaluate the resulting discriminant functions, the percentage of correct classification of individuals into sampling areas was calculated using jacknife cross-validation (Klecka, 1980) and compared to those obtained from random distribution.

Moreover, the performance of the discriminant analyses was assessed using the Wilks' λ. This value is the ratio between the intra-group variance and the total variance, and provides an objective way of calculating the percentage of agreement between real and predicted groups' membership. Wilks' λ values range from 0 to 1 and the closer to 0, the better the discriminating power of the RDA. To complete the stock identification procedure, a cluster analysis according to Ward's hierarchical agglomerative algorithm based on squared Euclidean distances was performed on the residual shape matrix R_S to group individuals with similar otolith shapes. These analyses were carried out three times: on left otoliths only, on right otoliths only and on both.

Statistical analyses were performed using the following packages in the statistical environment R (R Development Core Team, 2016): 'nlme' (Pinheiro *et al.*, 2016), 'Effects' (Fox, 2003), 'Vegan' (Oksanen *et al.*, 2013), 'SP' (Bivand *et al.,* 2013), 'ggplot2' (Wickham, 2016), 'RGEOS' (Bivand *et al.,* 2013), 'MASS' (Venables and Ripley, 2002) and 'RRCOV' (Todorov and Filzmoser, 2009).

RESULTS

Directional asymmetry in otolith shape

Among the 99 Fourier harmonics extracted to describe individual otolith contours, the first 26 harmonics explained at least 99.99% of the variation in otolith contour of each individual and were thus used for further analysis. After PCA on the EFD's, only the first six PC's were kept for the shape matrix S according to the broken-stick model (which, in this case, corresponded to a threshold of 2.4% of the total variance explained; Borcard *et al.*, 2011). These 6 PC's explained 78% of the total variance in the EFD's.

The multivariate mixed-effects model on the shape matrix S showed that there was a significant DA between left and right otolith shape at the global scale (Table 2, SI effect) with a consistent bias towards the right side (Supplementary Figure S1). The amplitude of DA, measured as the percentage of the non-overlapping surface between the right

and left otolith shapes, was on average equal to 2.77% among all sampling sites. However, there was also a significant effect of the interaction between side and sampling location on otolith shape (Table 2; $SI:LO$ effect) indicating that the amplitude and/or the direction of DA varied across sampling locations. More precisely, the amplitude of DA varied between 1.25% and 4.66% depending on the sampling site (Fig. 2) and was significant in only 5 of them, located along the Algerian and Italian coasts. The main shape difference between left and right otoliths was located between the rostrum and the antirostrum has shown by average left and right otoliths shape reconstruction at each sampling location (Fig. 2). In addition to its amplitude, the direction of DA also varied according to the considered location (Fig. 2). Among the sampling locations with a significant DA, the right otolith presented a width/length ratio larger than the left one in the Ligurian and Tyrrhenian Seas whereas it was the reverse in the Gulfs of Oran, Bejaia and Annaba (Fig. 2; Supplementary Table S1).

Fine-grained geographical structuring of otolith shape

The effect of sampling location on otolith shape was significant in the multivariate mixed effects model (Table 2, LO effect) suggesting geographical variation in otolith shape that could used to discriminate individuals from different geographical origins. Sampling location was therefore used as an explanatory variable in the subsequent otolith shape-based LDA. In contrast with the previous analyses, the procedure to produce the otolith shape matrix S was performed separately for left and right otoliths. The first six PC's after PCA on the first 26 harmonics EFD's were selected for the corresponding left and right shape matrices S_L and S_R. After removal of the effect of individuals' total length L by a RDA on S_L and S_R to obtain residual shape matrices R_{S_L} and R_{S_R}, the overall jacknifed classification success of the LDA was 37% for the left otoliths and 39% for the right ones (Tables 3 and 4). The analysis confirmed significant differences between sampling sites for otoliths of both sides (left otoliths: Wilks' λ = 0.426; F_{2860}^{60} = 10.13; p<0.001; right otoliths: Wilks' λ = 0.351; F_{2860}^{60} = 12.97; p<0.001). For left otoliths, the misclassified

individuals were distributed across all locations (Table 3) whereas, for right otoliths, they were segregated between two main groups: N-W Mediterranean Sea *versus* other locations (Table 4).

Clustering on otolith shape

The hierarchical clustering analysis identified three clusters for left and right otoliths (Table 5). No geographical coherence was identified for the three clusters of the left otoliths (Table 5). However, for right otoliths, the predicted areas coincided with 1) the north-western part of the Mediterranean Sea (Gulf of Lions, Corsica, Northern Ligurian Sea and Southern Ligurian Sea), 2) a large continuum composed of the central-eastern Atlantic Ocean (Tenerife Island) and the South-Wwestern part of Mediterranean Sea (Gulfs of Oran, Bejaia, Annaba and Tunis) and 3) the eastern part of the Mediterranean Sea (Ionian Sea and Aegean Sea) (Table 5). The same analyses as above were repeated but using the shape of otoliths of both sides at the same time. The results corroborated those obtained when using the right otoliths only. Firstly, the overall jacknifed classification success was 39%, similar to the one obtained with the right otoliths (Supplementary Table S2; Table 4). Secondly, the hierarchical clustering analysis identified the same 3 geographically coherent clusters (Supplementary Table S2; Table 5)

Stock structure inferred from otolith shape

The stock structure was investigated using right and left otoliths together. Combining the geographical areas into two stocks, the North-Western Mediterranean Sea and the rest consisting of the Atlantic Ocean and the South-Western Mediterranean Sea, 72% of individuals were assigned correctly by the LDA. However, the overall classification success was the same when integrating the Central and Eastern Mediterranean Sea (Gulf of Tunis, Aegean and Ionian Seas) in either of the two previous stocks. The best overall classification success (Wilks' λ = 0.525; F_{1106}^{12}=40.13; p-value<0.001; Correct classification rate = 86%) was obtained with 3 stocks units consisting in:

317 - the North-Western Mediterranean Sea (from the Gulf of Lions to the Tyrrhenian Sea),
318 - the Central-Eastern Atlantic Ocean and South-Western Mediterranean Sea (from the
319 Canary Islands to Gulf of Tunis), and
320 - the Eastern Mediterranean Sea (from the Ionian Sea to Aegean Sea).
321 The otoliths from the North-Western Mediterranean Sea presented a lower width/length
322 ratio than that of the otoliths from the southern part of the Mediterranean Sea and the
323 Atlantic Ocean. The otoliths from the Eastern Mediterranean Sea were closer to those
324 from the southern part of the Mediterranean Sea than to those from the North-Western
325 Mediterranean Sea in terms of shape (Figure 3). This split into 3 stocks using both right
326 and left otoliths dataset together was also coherent when using right otoliths' shape
327 (Wilks' λ = 0.627; F_{1106}^{12}=31.71; p-value<0.001; Correct classification rate= 75%),
328 whereas it was not when left otoliths' shape (Wilks' λ = 0.741; F_{1106}^{12}=30.45; p-
329 value=0.081, Correct classification rate = 47%).

330

331 **DISCUSSION**

332 ***Effect of confounding factors on the otolith shape***

333 The otolith shape of fish from different geographical origins is affected by both abiotic
334 environmental parameters (e.g. temperature, salinity) and biotic parameters such as prey
335 availability, and is dependent on individual genotype (Campana and Casselman, 1993;
336 Cadrin and Friedland, 1999; Torres *et al.*, 2000; Cardinale *et al.*, 2004; Gagliano and
337 McCormick, 2004; Swan *et al.*, 2006; Vignon and Morat, 2010). Consequently, a
338 combination of both environmental and genetic variation generates the morphological
339 differences in otolith shape that may allow the discrimination of stock units. However, the
340 factors that influence the shape are not fully understood and have not been investigated
341 deeply yet (Burke *et al.*, 2008). A recent study showed that the ontogenetic trajectory of
342 otolith shape could be affected by the environmental disturbance during early life stage
343 (Vignon, 2018). Other studies have attributed shape differences to fish length (Smith,

1992; Campana and Casselman, 1993; Mérigot *et al.*, 2007), age (Bird *et al.*, 1986), year-class (Castonguay *et al.*, 1991; Campana and Casselman, 1993; Bolles and Begg, 2000; Mapp *et al.*, 2017), sexual maturity (Campana and Casselman, 1993; Cardinale *et al.*, 2004) and sexual dimorphism (Campana and Casselman, 1993; Bolles and Begg, 2000). More specifically, otolith shape has been reported to be related to fish growth and thus subsequently size (e.g. Campana and Casselman, 1993). Furthermore, ontogenic changes in otolith shape, also often measured as size-related variation, have been shown to arise from variability in growth rates depending on habitat quality and the developmental processes (Simoneau *et al.* 2000, Monteiro *et al.,* 2005). Additionally, the formation of a secondary growth centre and/or the appearance of checks in response to stress conditions can modify the otolith shape and the level of crenulation during the early life stages (Campana and Nielson, 1985; Massou *et al.*, 2004; Hüssy, 2008; Vignon, 2018). Consequently, the complexity of the otolith outline increases with the ontogenetic stage of the fish. To limit this effect, sampling can be restricted to a specific life-stage and/or to a narrow length range. If these factors are not taken into account, results of otolith shape-based stock discrimination might be biased. This is the reason why all analyses in this study were carried out on adults of two to four years old within a limited size range. In addition, the effect of individuals' total length was systematically accounted for.

Directional bilateral asymmetry in otolith shape

Our results show that DA can be observed in otolith shape in roundfishes such as bogue. DA between right and left otolith shapes was previously described for other roundfish species such as *Liza ramada* (Rebaya *et al.,* 2017), *Diplodus annularis* (Trojette *et al.,* 2015), *Diplodus puntazzo* (Bostanci *et al.,* 2016), *Clupea harengus* (Bird *et al.,* 1986) and *Scomberomorus niphonius* (Zhang *et al.,* 2016). Conversely, symmetry between left and right otolith shapes was observed for other fish species: *Gadus morhua* (Cardinale *et al.,* 2004; Petursdottir *et al.,* 2006), *Synechogobius ommaturus* (Wang *et al.,* 2011), *Coryphaena hippurus* (Duarte-Neto *et al.,* 2008), *Xiphias gladius* (Mahé *et al.,* 2016),

372 *Scomber scombrus* (Castonguay *et al.,* 1991), and *Lutjanus kasmira* (Vignon and Morat,
373 2010). Although these studies tested for DA in roundfishes (and sometimes detected),
374 they never studied it in detail.
375 DA has also been reported for flatfish species, such as *Solea solea* (Merigot *et al.*, 2007;
376 Mille et al., 2015), *Limanda limanda* and *Lepidorhombus whiffiagonis* (Mille *et al.,* 2015).
377 Otolith DA is expected in flatfishes and could arise during their early life, particularly after
378 the cranial deformation and the migration of one eye to the other side caused by cell
379 proliferation in suborbital tissue during metamorphosis at the larval stage (Bao *et al.,*
380 2011). This lateralization process may induce the difference in otolith biomineralisation
381 (carbonate accretion rates) often observed between the two inner ears of flatfishes, with
382 the blind side generally growing faster in length and weight than the eyed side (Sogard,
383 1991; Fischer and Thompson, 2004; Helling *et al.,* 2005, Mille *et al.,* 2015).
384 In contrast, in bilaterally symmetrical organisms, i.e., most vertebrates including
385 roundfishes, symmetry is expected to be the rule and to be maintained by homeostasis
386 processes (Palmer, 2009). Deviations from bilateral symmetry in roundfish otolith shape
387 have been reported as potentially resulting from FA and/or DA (Lemberget and
388 Mccormick, 2009; Lychakov, 2013). The origin and consequences of otolith FA on fish
389 remain largely unknown and debated (Diaz *et al.*, 2015), although it has been
390 documented in several fish species and is regularly associated with stress and/or
391 environmental heterogeneity and thus thought as an indicator of developmental
392 instability (Downhower *et al.*, 1990; Lemberget and Mccormick, 2009, Green *et al.*,
393 2017). Lemberget and McCormick (2009) supported that otolith FA could be considered
394 as a sensitive indicator of fish health that directly affects the fish performance because
395 otoliths are essential to balance and hearing. More studies need to be carried out to
396 improve the understanding of otolith FA, including its sources and effects.
397 Regarding DA, which is a consistent bias towards one side, even less is known regarding
398 its potential origin in roundfishes. Although it has been observed in some previous
399 studies, it was only considered as a nuisance in otolith shape analysis and not

400 considered further. Specifically, there was no study trying to identify potential
401 geographical or phylogenetic patterns in otolith DA in roundfishes. The present study
402 shows that DA can be observed for one roundfish species in some geographical areas,
403 whereas it is not in others. In addition, the direction of DA can change according to the
404 geographical area where it is detected. Although it is difficult to say whether these results
405 could be generalized to other roundfish species, they suggest that variability in otolith DA
406 in bogue at least could be related to population geographical structuration and thus could
407 be a phenotypically plastic response to environmental drivers, such as temperature,
408 current patterns and food availability, and/or result from genetic differentiation between
409 geographical locations.
410 Whether varying DA across geographical location results from adaptive or passive
411 phenotypic plasticity and/or adaptive or neutral genetic differentiation is then an open
412 question. Otolith shape asymmetry, be it FA or DA, could generate some dysfunction of
413 the vestibular sensing (Hilbig *et al.*, 2011). Notably, otolith asymmetry affects the
414 acoustic functionality (sensitivity, temporal processing and sound localization) (Lychakov
415 and Rebane, 2005; Lychakov *et al.,* 2008) and is related to kinetotic swimming of fish
416 (aberrant movement pattern or static space sickness) (Anken *et al.,* 1998; Beier *et al.,*
417 2002; Hilbig *et al.,* 2003; Hilbig *et al.,* 2011). In contrast, no obvious advantage of otolith
418 asymmetry has been put forward in the literature, which suggests that, be it of plastic or
419 genetic origin, otolith DA in roundfishes could be non-adaptive.
420 ***Stock structure of bogue in the Mediterranean Sea and the Atlantic Ocean***
421 The stock structure revealed by shape analysis of the right otoliths was similar to that
422 obtained when using otoliths from both sides. Three different stocks were identified:
423 North-Western Mediterranean Sea (from the Gulf of Lions to the Tyrrhenian Sea),
424 Central-Eastern Atlantic Ocean and South-Western Mediterranean Sea (from the Canary
425 Islands to the Gulf of Tunis) and Eastern Mediterranean Sea (from the Ionian Sea to the
426 Aegean Sea). This stock structure is similar to that observed for other species in the
427 same areas such as sardine or cephalopods (see Jemaa *et al.,* 2015; Keller *et al.,* 2017).

Ider *et al.* (2017) analyzing only the data from the Algerian coasts, identified only one stock for this area just as the present study conducted at much larger geographic scale, which indicates consistency of otolith shape-based stock discrimination across multiple geographic scales. Factors structuring bogue stocks at the level of the Mediterranean region seem to be linked to environmental features, notably physical oceanographic characteristics of the studied area. The Mediterranean Sea presents a complex circulation pattern. In the South-Western Mediterranean Sea, the environmental conditions are directly influenced by oceanographic processes (Catalan *et al.,* 2013) with the entrance of the Atlantic current being the main forcing agent modulating hydrological processes (Garcia-Lafuente *et al.,* 1998). This exchange of water masses creates the Almeria-Oran front, with Atlantic water entering the Mediterranean Sea at the surface (up to 150–200m), and generates a strong current that feeds the Algerian current. This circulation pattern could explain the presence of one stock unit from the Canary Islands to the Algerian coast and its isolation from one stock unit in the North-Western Mediterranean Sea, the latter being also under the influence of the Northern current. The Sicily Channel is a known physical barrier between the western and the eastern basins of the Mediterranean Sea because of its relatively low depth and its peculiar circulation pattern. Regarding the latter, it is under the mixed influence of the Atlantic Ocean current in the western part and, conversely, of the Levantine Intermediate Water current (LIW), which moves water masses from east to west, in the eastern part (Skliris, 2014). This would explain the separation of the eastern Mediterranean stock from the two more western ones. On top of the hydrological regime, variations in environmental conditions are also likely to play a major role in the observed differences in otolith shape within the studied geographic areas. Water temperature is a key factor influencing primary production in the Mediterranean Sea and these two factors combined are important drivers of fish growth. The average annual sea surface temperature (SST from 2013 to 2016, sampling period, Supplementary Figure S3) exhibited a clear gradient between the northwestern and the southeastern parts of the Mediterranean Sea with higher values

along the Levantine coast (Shaltout and Omstedt, 2014). Conversely, primary production (measured as average annual chlorophyll-a concentration) decreased along a gradient from the North-Western Mediterranean Sea characterized by oligotrophic waters to the southeastern Mediterranean Sea identified as ultraoligotrophic waters (Supplementary Figure S4; Stambler, 2014). As for the circulation pattern, the Sicily Channel stands out as a transition zone in terms of environmental conditions. It is characterized by intermediate temperatures (Supplementary Figure S2) and a mix of high primary production along the Tunisian coasts, and more specifically in the Gulf of Gabes, and low primary production in the rest of the Channel (Supplementary Figure S3), which generates some variations of the food web in the area (Rumolo *et al.,* 2017). The higher rate of misclassification of fish sampled in Tunisia is likely to result from the transitional nature of the Sicily Channel in terms of circulation and environmental conditions.

These results highlight the importance of taking into account potential otolith DA when using otolith shape analysis for fish stock identification. Our analyses suggest that there are 3 bogue stocks in the study area that are geographically coherent and make sense relative to the circulation pattern and environmental conditions in the Mediterranean Sea when using right otoliths or otoliths of both sides together, whereas no population structuration is found when using left otoliths. These results about bogue population structure would need to be confirmed by further studies including genetic analyses of specimens included in the otolith shape analysis and/or otolith microchemistry.

SUPPLEMENTARY DATA

Supplementary material is available at the ICESJMS online version of the manuscript.

ACKNOWLEDGEMENTS

We would especially thank Willie Mc Curdy (Northern Ireland) and Joanne Smith (UK England), for their valuable help in editing this manuscript.

REFERENCES

Anken, R., Kappel, T., and Rahmann, H. 1998. Morphometry of fish inner ear otoliths after Development at 3g hypergravity. Acta Oto-Laryngologica, 118: 534–539.

Bao, B., Ke, Z., Xing, J., Peatman, E., Liu, Z., Xie, C., Xu, B., Gai, J., Gong, X., Yang, G., Jiang, Y., Tang, W., and Ren, D. 2011. Proliferating cells in suborbital tissue drive eye migration in flatfish. Developmental Biology, 351: 200–207.

Begg, G. A., and Brown, R. W., 2000. Stock identification of haddock *Melanogrammus aeglefinus* on Georges Bank based on otolith shape analysis. Transactions of the American Fisheries Society, 129: 935–945.

Beier, M., Anken, R., and Rahmann, H. 2002. Susceptibility to abnormal (kinetotic) swimming in fish correlates with inner ear carbonic anhydrase-reactivity. Neuroscience Letter, 335: 17–20.

Benzinou, A., Carbini, S., Nasreddine, K., Elleboode, R., and Mahé, K. 2013. Discriminating stocks of striped red mullet (*Mullus surmuletus*) in the Northwest European seas using three automatic shape classification methods. Fisheries Research, 143: 153–160.

Bird, J. L., Eppler, D. T., and Checkley, D. M. 1986. Comparisons of herring otoliths using Fourier series shape analysis. Canadian Journal of Fisheries and Aquatic Sciences, 43: 1228–1234.

Bivand, R. S., Pebesma, E., and Gomez-Rubio, V. 2013. Applied spatial data analysis with R, Second edition. Springer, New York. 405 pp.

Borcard, D., Gillet, F., and Legendre, P. 2011. Numerical Ecology with R. Springer, New York Dordrecht London Heidelberg. 306 pp.

Bolles, K. L., and Begg, G. A. 2000. Distinction between silver hake (*Merluccius bilinearis*) stocks in U.S. waters of the northwest Atlantic using whole otolith morphometric. Fishery Bulletin, 98: 451–462.

508 Bostanci, D., Yilmaz, M., Yedier, S., Kurucu, G., Kontas, S., Darçin, M., and Polat, N.
509 2016. Sagittal otolith morphology of sharpsnout seabream *Diplodus puntazzo* (Walbaum,
510 1792) in the Aegean sea. International Journal of Morphology, 34(2): 484–488.
511 Boudinar, A. S., Chaoui, L., Mahé, K., Cachera, M., and Kara, M. H., 2015. Habitat
512 discrimination of big-scale sand smelt *Atherina boyeri* Risso, 1810 (Atheriniformes:
513 Atherinidae) in eastern Algeria using somatic morphology and otolith shape, Italian
514 Journal of Zoology, 82: 446–453.
515 Bouke N., Brophy D., and King P. 2008. Otolith shape analysis: its application for
516 discriminating between stocks of Irish Sea and Celtic Sea herring (*Clupea harengus*) in
517 the Irish Sea. ICES Journal of Marine Science, 65(9): 1670–1675.
518 Cadrin S. X., Kerr, L. A., and Mariani, S. 2014. Stock Identification Methods: Applications
519 in Fishery Science. 2nd edn, Elsevier Academic Press, Amsterdam. 566 pp.
520 Cadrin, S. X., and Friedland, K. D. 1999. The utility of image processing techniques for
521 morphometric analysis and stock identification. Fisheries Research, 43: 129–139.
522 Campana, S. E. 1999. Chemistry and composition of fish otoliths: pathways,
523 mechanisms and applications. Marine Ecology Progress Series, 188: 263–297.
524 Campana, S.E., and Casselman, J. M. 1993. Stock discrimination using otolith shape
525 analysis. Canadian Journal of Fisheries and Aquatic Sciences, 50: 1062–1083.
526 Capoccioni, F., Costa, C., Aguzzi, J., Menesatti, P., Lombarte, A., and Ciccotti, E. 2011.
527 Ontogenetic and environmental effects on otolith shape variability in three Mediterranean
528 European eel (*Anguilla anguilla*, L.) populations. Journal of Experimental Marine Biology
529 and Ecology, 397: 1–7.
530 Cardinale, M., Doerin-Arjes, P., Kastowsky, M., and Mosegaard, H. 2004. Effects of sex,
531 stock, and environment on the shape of known-age Atlantic cod (*Gadus morhua*) otoliths.
532 Canadian Journal of Fisheries and Aquatic Sciences, 61: 158–167.
533 Campana, S.E., and Neilson, J.D. 1985. Microstructure of fish otoliths. Canadian Journal
534 of Fisheries and Aquatic Sciences, 42: 1014–1032.

535 Casselman, J. M. 1987. Determination of age and growth. *In* The Biology of Fish Growth,
536 pp. 209-242. Ed. by A. H. Weatherley and H. S. Gill. Academic Press, New York. 443
537 pp.

538 Castonguay, M., Simard, P., and Gagnon, P. 1991. Usefulness of Fourier analysis of
539 otolith shape for Atlantic mackerel (*Scomber scombrus*) stock discrimination. Canadian
540 Journal of Fisheries and Aquatic Sciences, 48: 296–302.

541 Catalan, I. A., Macias, D., Sole, J., Ospina-Alvarez, A., and Ruiz, J. 2013. Stay off the
542 motorway: resolving the pre-recruitment life history dynamics of the European anchovy
543 in the SW Mediterranean through a spatially-explicit individual-based model (SEIBM).
544 Progress in Oceanography, 111: 140–153.
545 De Pontual, H., and Prouzet, P. 1987. Atlantic salmon (*Salmo salar* L.) stock
546 discrimination by scale shape analysis. Aquaculture and Fisheries Management, 18:
547 227-289.
548 De Pontual, H., and Prouzet, P. 1988. Numerical analysis of scale morphology to
549 discriminate between atlantic salmon stocks. Aquatic Living Resources, 1: 17-27.
550 Dimarchopoulou, D., Stergiou, K. I., and Tsikliras, A. C. 2017. Gap analysis on the
551 biology of Mediterranean marine fishes. PLoS ONE, 12(4): e0175949.
552 Díaz-Gil, C., Palmer, M., Catalán, I. A., Alós, J., Fuiman, L. A., García, E., del Mar Gil,
553 M. Grau, A., Kang, A., Maneja, R. H., Mohan, J. A., Morro, B., Schaffler, J. J., Buttay, L.,
554 Inmaculada, R. B. Borja, T., and Morales-Nin, B. 2015. Otolith fluctuating asymmetry: a
555 misconception of its biological relevance? ICES Journal of Marine Science, 72(7): 2079–
556 2089.
557 Dowhower, J. F., Blumer, L. S., Lejeune, P., Gaudin, P., Marconato, A., and Bisazza, A.
558 1990. Otolith asymmetry in *cottus bairdi* and *cottus gobio*. Polskie Archiwum
559 Hydrobiologii, 37(1-2): 209–220.

560 Duarte-Neto, P., Lessa, R., Stosic, B., and Morize, E. 2008. The use of sagittal otoliths
561 in discriminating stocks of common dolphinfish (*Coryphaena hippurus*) off northeastern
562 brazil using multishape descriptors. ICES Journal of Marine Science, 65(7): 1144–1152.
563 FAO 2016. The State of Mediterranean and Black Sea Fisheries 2016 (SoMFi 2016),
564 Food and Agriculture Organization of the United Nations, Rome. 152 pp.
565 Fischer, A. J., and Thompson, B. A. 2004. The age and growth of southern flounder,
566 *Paralichthys lethostigma*, from Louisiana estuarine and offshorewaters. Bulletin of
567 Marine Science, 75: 63–77.
568 Fox, J. 2003. Effect Displays in R for Generalised Linear Models. Journal of Statistical
569 Software, 8(15): 1-18.
570 Fox, J., and Weisberg, S. 2011. An {R} Companion to Applied Regression, 2nd edn,
571 Thousand Oaks CA. 472 pp.
572 Gagliano, M., and McCormick, M. I. 2004. Feeding history influences otolith shape in
573 tropical fish. Marine Ecology Progress Series, 278: 291–296.
574 Garcia, A., Mattiucci, S., Damiano, S., Santos, M. N., and Nascetti, G. 2011. Metazoan
575 parasites of swordfish, *Xiphias gladius* (Pisces: Xiphiidae) from the Atlantic Ocean:
576 implications for host stock identification. ICES Journal of Marine Science, 68: 175–182.
577 García-Lafuente, J., Vargas, J. M., Cano, N., Sarhan, T., Plaza, F., and Vargas, M. 1998.
578 Observaciones de corriente en la estación 'N' en el Estrecho de Gibraltar desde Octubre
579 de 1995 a Mayo de 1996. Informes Técnicos. Instituto Español de Oceanografía, 169:
580 1-46.
581 Green, A. A., Mosaliganti, K. R., Swinburne, I. A., Obholzer, N. D., and Megason, S. G.
582 2017. Recovery of Shape and Size in a Developing Organ Pair. Developmental
583 Dynamics, 246: 451–465.
584 Helling, K., Scherer, H., Hausmann, S., and Clarke, A. H. 2005. Otolith mass
585 asymmetries in the utricle and saccule of flatfish. Journal of Vestibular Research, 15:
586 59–64.

587 Hilbig, R. Knie, M., Shcherbakov, D., and Anken, R. H. 2011. *Analysis of Behaviour and*
588 *Habituation of Fish Exposed to Diminished Gravity in Correlation to Inner Ear Stone*
589 *Formation – A Sounding Rocket Experiment (TEXUS 45).* Proceedings of the 20th ESA
590 Symposium on European Rocket and Balloon Programmes and Related Research, 22–
591 26 May 2011, Hyere, France.
592 Hilbig, R., Anken, R., and Rahmann, H. 2003. On the origin of susceptibility to kinetotic
593 swimming behaviour in fish: A parabolic aircraft flight study. Journal of Vestibular
594 Research, 12: 185–189.
595 Hüssy, K. 2008. Otolith shape in juvenile cod (*Gadus morhua*): ontogenetic and
596 environmental effects. Journal of Experimental Marine Biology and Ecology, 364: 35–41.
597 Hutchings, J. A. 2005. Life history consequences of overexploitation to population
598 recovery in Northwest Atlantic cod (*Gadus morhua*). Canadian Journal of Fisheries and
599 Aquatic Sciences, 62: 824–832.
600 Govind, C. K., & Pearce, J. 1986. Differential Reflex Activity Determines Claw and Closer
601 Muscle Asymmetry in Developing Lobsters. Science, 233: 354–356
602 ICES 2016. Report of the Stock Identification Methods Working Group (SIMWG). ICES
603 CM 2016/SSGEPI:16. 47 pp.
604 Ider, D., Ramdane, Z., Mahé, K., Dufour, J. L., Bacha, M., and Amara, R., 2017. Use of
605 otolith shape analysis to discriminate stocks of *Boops boops* (L.) from the Algerian coast
606 (southwestern part of the Mediterranean Sea). African Journal of Marine Science, 39(3):
607 251-258.

608 Jemaa, S., Bacha, M., Khalaf, G., Dessailly, D., Rabhi, K., and Amara, R. 2015. What
609 can otolith shape analysis tell us about population structure of the European sardine,
610 *Sardina pilchardus*, from Atlantic and Mediterranean waters? Journal of Sea Research,
611 96: 11–17.
612 Keller, S., Quetglas, A., Puerta, P., Bitetto, I., Casciaro, L., Cuccu, D., Esteban, A.,
613 Garcia, C., Garofalo, G., Guijarro, B., Josephides, M., Jadaud, A., Lefkaditou, E.,

614 Maiorano, P., Manfredi, C., Marceta, B., Micallef, R., Peristeraki, P., Relini, G., Sartor,
615 P., Spedicato, M. T., Tserpes, G., and Hidalgo, M. 2017. Environmentally driven
616 synchronies of Mediterranean cephalopod populations. Progress In Oceanography, 152:
617 1–14.
618 Klecka, W. R. 1980. Discriminant analysis. Sage Publications, Beverly Hills.
619 Kuhl, F., and Giardina, C. 1982. Elliptic Fourier features of a closed contour. Computer
620 Graphics and Image Processing, 18: 236–258.
621 Legendre, P., and Legendre, L. F. J. 1998. Numerical Ecology. 2nd edn, Elsevier
622 Science. 853 pp.
623 Lemberget, T., and Mccormick, M. I. 2009. Replenishment success linked to fluctuating
624 asymmetry in larval fish. Oecologia, 159: 83–93.
625 Lestrel, P. E. 2008. Fourier Descriptors and their Applications in Biology. Cambridge
626 University Press, Cambridge. 460 pp.
627 Lombarte, A., and Lleonart, J. 1993. Otolith size changes related with body growth,
628 habitat depth and temperature. Environmental Biology of Fishes, 37: 297–306.
629 Lychakov, D. 2013. Behavioral lateralization and otolith asymmetry. Journal of
630 Evolutionary Biochemistry and Physiology, 49: 441–456.
631 Lychakov, D. V., and Rebane, Y. T. 2005. Fish otolith mass asymmetry: Morphometry
632 and influence on acoustic functionality. Hearing Research, 201: 55–69.
633 Lychakov, D. V., Rebane, Y. T., Lombarte, A., Demestre, M., and Fuiman, L. A. 2008.
634 Saccular otolith mass asymmetry in adult flatfishes. Journal of Fish Biology, 72: 2579–
635 2594.
636 Mahé, K., Evano, H., Mille, T., Muths, D., and Bourjea, J. 2016. Otolith shape as a
637 valuable tool to evaluate the stock structure of swordfish *Xiphias gladius* in the Indian
638 Ocean. African Journal of Marine Science, 38(4): 457–464.
639 Mapp, J., Fisher, M., Bagnall, A., Lines, J., Warne S., and Phillips, J. S. 2013. *Clupea*
640 *Harengus*: Intraspecies Distinction using Curvature Scale Space and Shapelets-
641 Classification of North-sea and Thames Herring using Boundary Contour of Sagittal

642 Otoliths. Proc. 2nd International Conference on Pattern Recognition Applications and
643 Methods (ICPRAM 2013)
644 Mapp, J., Hunter, E., Van Der Kooijc, J., Songer, S., and Fisher, M. 2017. Otolith shape
645 and size: The importance of age when determining indices for fish-stock separation.
646 Fisheries Research, 190: 43–52.
647 Massou A.M., Le Bail P.Y., Panfili J., Laë R., Baroiller J.F., Mikolasek O., Fontenelle G.
648 and Auperin B. 2004 Effects of confinement stress of variable duration on the growth and
649 microincrement deposition in the otoliths of *Oreochromis niloticus* (Cichlidae). Journal of
650 Fish Biology, 65:1253-1269.
651 Mérigot, B., Letourneur, Y., and Lecomte-Finiger, R. 2007. Characterization of local
652 populations of the common sole *Solea solea* (Pisces, Soleidae) in the NW Mediterranean
653 through otolith morphometrics and shape analysis. Marine Biology, 151: 997–1008.
654 Mille, T., Mahé, K., Cachera, M., Villanueva, C. M., De Pontual, H., and Ernande, B.
655 2016. Diet is correlated with otolith shape in marine fish. Marine Ecology Progress
656 Series, 555: 167–184.
657 Mille, T., Mahé, K., Villanueva, C. M., De Pontual, H., and Ernande, B. 2015. Sagittal
658 otolith morphogenesis asymmetry in marine fishes. Journal of Fish Biology, 87: 646–663.
659 Monteiro, L. R., Di Beneditto, A. P. M., Guillermo, L. H., and Rivera, L. A. 2005. Allometric
660 changes and shape differentiation of sagitta otoliths in sciaenid fishes. Fishery Research,
661 74: 288–299.
662 Monteiro, P., Bentes, L., Coelho, R., Correia, C., Gonçalves, J., Lino, P. G., Ribeiro, J.,
663 and Erzini, K. 2006. Age and growth, mortality, reproduction and relative yield per recruit
664 of the bogue, *Boops boops* Linné, 1758 (Sparidae), from the Algarve (south of Portugal)
665 longline fishery. Journal of Applied Ichthyology, 22 (5): 345–352.
666 Oksanen, J., Blanchet, F. G., Kindt, R., Legendre, P., Minchin, P. R., O'Hara, R. B.,
667 Simpson, G. L., Solymos, P., Stevens, H. M. H., and Wagner, H. 2013. Vegan:
668 Community Ecology Package. R package version 2.0–10. 292 pp.
669 Palmer, A. R. 2009. Animal asymmetry. Current Biology, 19: 473–477.

670 Palmer, A. R., & Strobeck, C. 1986 Fluctuating Asymmetry: Measurement, Analysis,
671 Patterns. Annual Review of Ecology and Systematics, 17: 391–421.
672 Palmer, A. R., & Strobeck, C. 1992. Fluctuating asymmetry as a measure of
673 developmental stability implications of non-normal distributions and power of statistical
674 tests. Acta Zoologica Fennica, 191: 57–72.
675 Parisi-Baradad, V., Lombarte, A., García-Ladona, E., Cabestany, J., Piera, J., and Chic,
676 Ò. 2005. Otolith shape contour analysis using affine transformation invariant wavelet
677 transforms and curvature scale space representation. Marine Freshwater Research, 56:
678 795–804.
679 Pawson, M. G., and Jennings, S. 1996. A critique of methods for stock identification in
680 marine capture fisheries. Fisheries Research, 25: 3–4.
681 Pestana, G., and Porteiro, C. 2009. Geographic variability of sardine dynamics in the
682 Iberian Biscay region. ICES Journal of Marine Science, 66: 495–508.
683 Petursdottir, G., Begg, G. A., and Marteinsdottir, G. 2006. Discrimination between
684 Icelandic cod (*Gadus morhua* L.) populations from adjacent spawning areas based on
685 otolith growth and shape. Fisheries Research, 80: 182–189.
686 Pinheiro, J., Bates, D., DebRoy, S., Sarkar, D. 2016. nlme: Linear and Nonlinear Mixed
687 Effects Models. R package version 3.1-128.
688 Pita, A., Casey, J., Hawkins, S. J., Villarreal, M., and Gutiérrez, M. J. 2016. Conceptual
689 and practical advances in fish stock delineation. Fisheries Research, 173(3): 185–193.
690 Ponton, D. 2006. Is geometric morphometrics efficient for comparing otolith shape of
691 different fish species?. Journal of Morphology, 267: 750–757.
692 R Development Core Team 2016. R: A language and environment for statistical
693 computing. R Foundation for Statistical Computing. Vienna, Austria.
694 Ramirez-Pérez, J. S., Quiñónez-Velázquez, C., García-Rodríguez, F. J., Felix-Uraga, R.,
695 and Melo-Barrera, F. N. 2010. Using the shape of sagitta otoliths in the discrimination of
696 phenotypic stocks in *Scomberomorus sierra* (Jordan and Starks, 1895). Canadian
697 Journal of Fisheries and Aquatic Sciences, 5: 82–93.

698 Rebaya, M., Ben Faleh, A. R., Allaya, H., Khedher, M., Trojette, M., Marsaoui, B.,
699 Fatnassi, M., Chalh, A., Quignard, J. P., and Trabelsi, M. 2017. Otolith shape
700 discrimination of *Liza ramada* (Actinopterygii: Mugiliformes: Mugilidae) from marine and
701 estuarine populations in Tunisia. Acta Ichthyologica et Piscatoria, 47(1): 13–21.
702 Reiss, H., Hoarau, G., Dickey-Collas, M., and Wolff, W. 2009. Genetic population
703 structure of marine fish: mismatch between biological and fisheries management units.
704 Fish and Fisheries, 10: 361–395.
705 Rencher, A. C., and Christensen, W. F. 2012. Methods of Multivariate Analysis. 3rd edn,
706 Wiley, New York. 800 pp.
707 Rohlf, F. J., and Archie, J. W. 1984. A Comparison of Fourier Methods for the Description
708 of Wing Shape in Mosquitoes (Diptera: Culicidae). Systematic Biology, 33: 302–317.
709 Rumolo, P., Basilone, G., Fanelli, E., Barra, M., Calabrò, M., Genovese, S., Gherardi, S.,
710 Ferreri, R., Mazzola, S., and Bonanno, A. 2017. Linking spatial distribution and feeding
711 behavior of Atlantic horse mackerel (*Trachurus trachurus*) in the Strait of Sicily (Central
712 Mediterranean sea). Journal of Sea Research, 121: 47–58.
713 Sadighzadeh, Z., Valinassab, T., Vosugi, G., Motallebi, A. A., Fatemi, M. R., Lombarte,
714 A., and Tuset, V. M. 2014. Use of otolith shape for stock identification of John's snapper,
715 *Lutjanus johnii* (Pisces: Lutjanidae), from the Persian Gulf and the Oman Sea. Fisheries
716 Research, 155: 59–63.
717 Shaltout, M., and Omstedt, A. 2014. Recent sea surface temperature trends and future
718 scenarios for the Mediterranean Sea. Oceanologia, 56(3): 411–443.
719 Silva, A., Skagen, D. W., Uriarte, A., Massé, J., Santos, M. B., Marques, V., Carrera, P.,
720 Beillois, P., Pestana, G., Porteiro, C., and Stratoudakis, Y. 2009. Geographic variability
721 of sardine dynamics in the Iberian Biscay region. ICES Journal of Marine Science, 66:
722 495–508.
723 Simoneau, M., Casselman, J. M., and Fortin, R. 2000. Determining the effect of negative
724 allometry (length/height relationship) on variation in otolith shape in lake trout (*Salvelinus*

725 *namaycush*), using Fourier-series analysis. Canadian Journal of Zoology, 78:
726 1597–1603.
727 Skliris, N. 2014. Past, present and future patterns of the thermohaline circulation and
728 characteristic water masses of the Mediterranean sea. *In* The Mediterranean Sea - its
729 History and Present Challenges, pp. 29-48. Ed. By S. Goffredo, and Z. Dubinky.D
730 Springer, Dordrecht, Heidelberg, New York, London. 678 pp.
731 Smith, M. K. 1992. Regional differences in otolith morphology of the deep slope red
732 snappers *Etelis carbunculus*. Canadian Journal of Fisheries and Aquatic Sciences, 49:
733 795–804.
734 Sogard, S. M. 1991. Interpretation of otolith microstructure in juvenile winter flounder
735 (*Pseudopleuronectes americanus*): ontogenetic development, daily increment validation,
736 and somatic growth relationships. Canadian Journal of Fisheries and Aquatic Sciences,
737 48: 1862–1871.
738 Stambler, N. 2014. The Mediterranean Sea – Primary Productivity *In* The Mediterranean
739 Sea - its History and Present Challenges, pp. 113-121. Ed. By S. Goffredo, and Z.
740 Dubinky.D Springer, Dordrecht, Heidelberg, New York, London. 678 pp.
741 Stephenson, R. L., Rodman, K., Aldous, D. G., and Lane, D. E. 1999. An in-season
742 approach to management under uncertainty: the case of the SW Nova Scotia herring
743 fishery. ICES Journal of Marine Science, 56: 1005–1013.
744 Swan, S. C., Geffen, A. J., Morales-Nin, B., Gordon, J. D. M., Shimmield, T., Sawyer, T.,
745 and Massutí, E. 2006. Otolith chemistry: an aid to stock separation of *Helicolenus*
746 *dactylopterus* (bluemouth) and *Merluccius merluccius* (European hake) in the Northeast
747 Atlantic and Mediterranean. ICES Journal of Marine Science, 63: 504–513.
748 Todorov, V. and Filzmoser P. 2009. An Object-Oriented Framework for Robust
749 Multivariate Analysis. Journal of Statistical Software, 32(3): 1-47.
750 Torres, G. J., Lombarte, A., Morales-Nin, B. 2000. Sagittal otolith size and shape
751 variability to identify geographical intraspecific differences in three species of genus
752 *Merluccius*. Journal of the Marine Biological Association of the UK, 80: 333–342.

753 Trojette, M., Ben Faleh, A., Fatnassi, M., Marsaoui, B., Mahouachi, N.H., Chalh, A.,
754 Quignard, J.-P., and Trabelsi, M. 2015. Stock discrimination of two insular populations
755 of *Diplodus annularis* (Actinop-terygii: Perciformes: Sparidae) along the coast of Tunisia
756 by analysis of otolith shape. Acta Ichthyologica Et Piscatoria, 45: 363–372.
757 Tuset, V.M., Lozano, I.J., Gonzalez, J.A., Pertusa, J.F., and Garcıa-Dıaz, M.M. 2003.
758 Shape indices to identify regional differences in otolith morphology of comber, *Serranus*
759 *cabrilla* (L., 1758). Journal of Applied Ichthyology, 19: 88–93.
760 Venables, W. N., and Ripley, B. D. 2002. Modern Applied Statistics with S, 4th edn,
761 Springer, New York. 446 pp.
762 Vergara-Solana, F. J., García-Rodríguez, F. J., and De La Cruz-Agüero, J. 2013.
763 Comparing body and otolith shape for stock discrimination of Pacific sardine, *Sardinops*
764 *sagax* Jenyns, 1842. Journal of Applied Ichthyology, 29: 1241–1246.
765 Vignon, M. 2018. Short-term stress for long-lasting otolith morphology – Brief
766 embryological stress disturbance can reorient otolith ontogenetic trajectory. Canadian
767 Journal of Fisheries and Aquatic Sciences, *In Press*
768 Vignon, M., and Morat, F. 2010. Environmental and genetic determinant of otolith shape
769 revealed by a non-indigenous tropical fish. Marine Ecology Progress Series, 411: 231–
770 241.
771 Wang, Y. J., Ye, Z. J., Liu, Q., and Cao, L. 2011. Stock discrimination of spotted tail goby
772 (*Synechogobius ommaturus*) in the Yellow Sea by analysis of otolith shape. Oceanologia
773 et Limnologia Sinica, 29: 192–198.
774 Whitehead, P. J. P., Bauchot, M. L., Hureau, J. C., Nielsen, J., and Tortonese, E. 1984.
775 Fishes of the North-eastern Atlantic and the Mediterranean, UNESCO, Paris, 510 pp.
776 Wickham, H. 2016. ggplot2: Elegant Graphics for Data Analysis. Springer-Verlag New
777 York.182 pp.
778 Wooster, W. S. 1992. King crab dethroned. *In* Climate, Variability, Climate Change and
779 Fisheries, pp. 14–30. Ed. by M. H. Glantz, Cambridge University Press, New York. 458
780 pp.

781 Zhang, C., Ye, Z., Li, Z., Wan, R., Ren, Y., and Dou, S. 2016. Population structure of
782 Japanese Spanish mackerel *Scomberomorus niphonius* in the Bohai Sea, the Yellow
783 Sea and the East China Sea: evidence from random forests based on otolith features.
784 Fisheries Science, 82: 251–256.

Figure 1 : Map of sampling locations of bogues (1: Tenerife Island; 2: Gulf of Oran, 3: Gulf of Bejaia, 4: Gulf of Annaba, 5: Gulf of Tunis, 6:Gulf of Lions , 7: Corsica Island, 8: Ligurian Sea, 9: Tyrrhenian Sea, 10: Ionian Sea, 11: Aegean Sea).

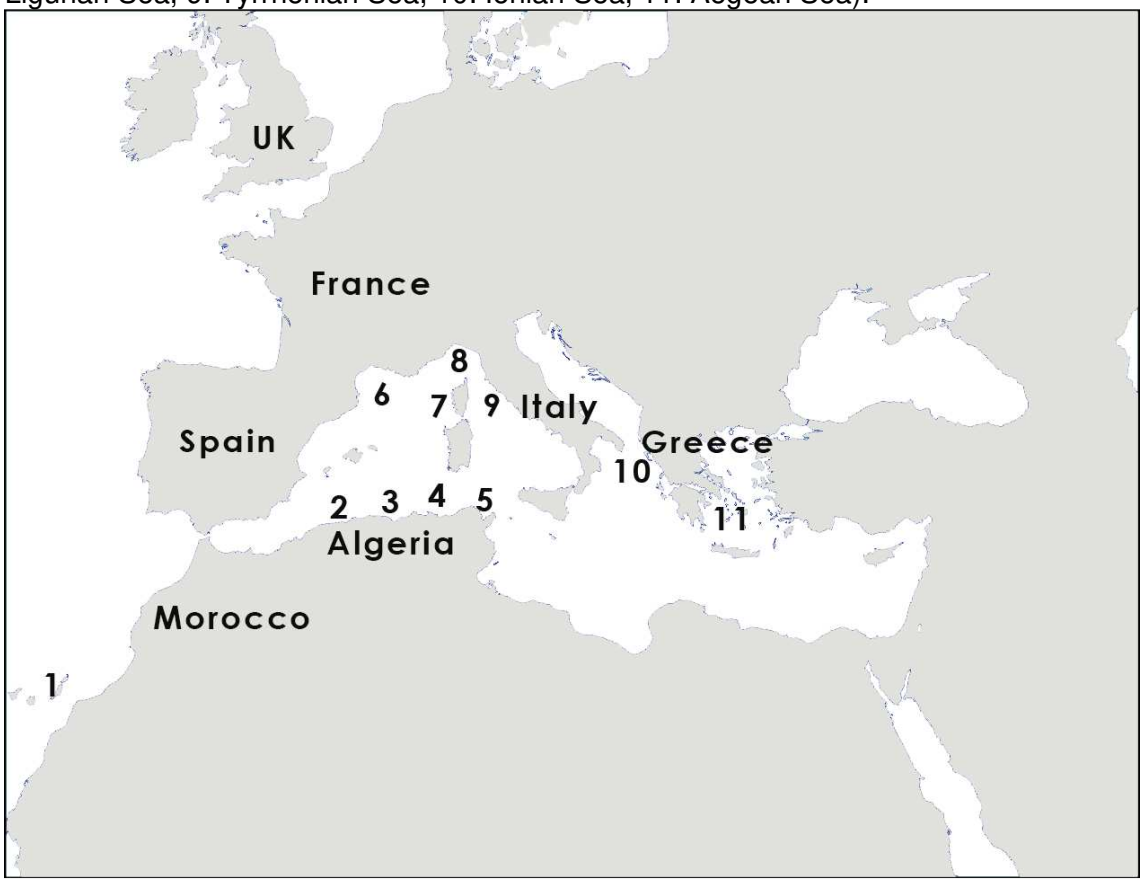

Figure 2: A) Directional asymmetry between left and right otolith shape at each sampling location as estimated by the interaction between side and sampling location in the multivariate mixed-effects model. Black dots and grey triangles represent the estimator for the left and right otolith, respectively, and vertical bars are there 95% confidence intervals. Percentage given in each panel is the average percentage of non-overlapping surface between the two reconstructed otolith shapes at the individual level. B) Difference between right (black line) and left (grey dotted line) otolith shape for each geographical location as shown by average shape reconstruction for each sampling location based on EFD's. Percentages are the average percentages of non-overlapping surface between the two reconstructed otolith shapes at the individual level (*<0.05).

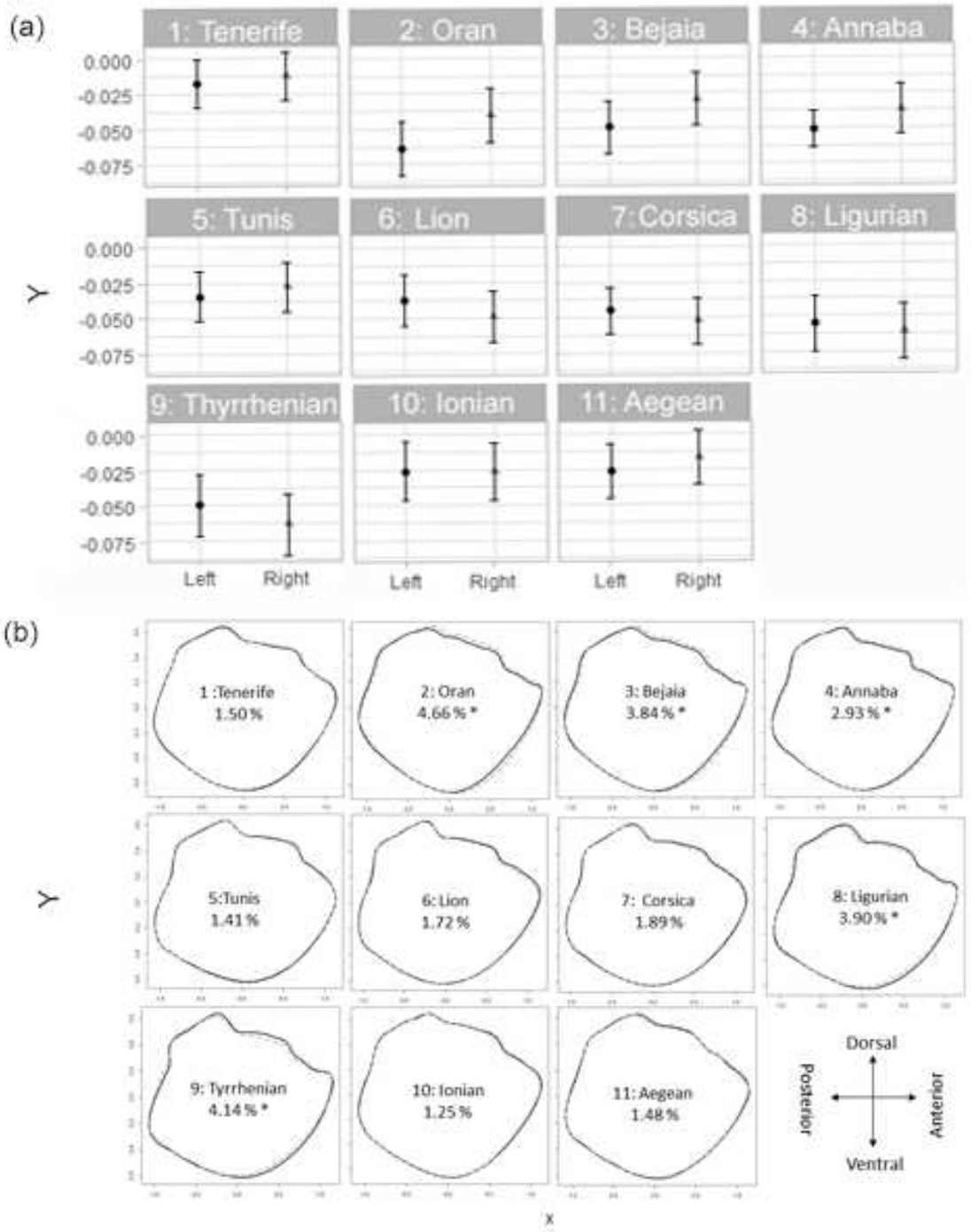

Figure 3: Difference among average reconstructed otolith shapes between the 3 identified stock units: Northwestern Mediterranean Sea (solid line; from the Gulf of Lions to the Tyrrhenian Sea), Eastern Mediterranean Sea (dashed line; from the Ionian Sea to the Aegean Sea) and Southwestern Mediterranean Sea and Atlantic Ocean (dotted line; from the Canary Islands to the Gulf of Tunis).

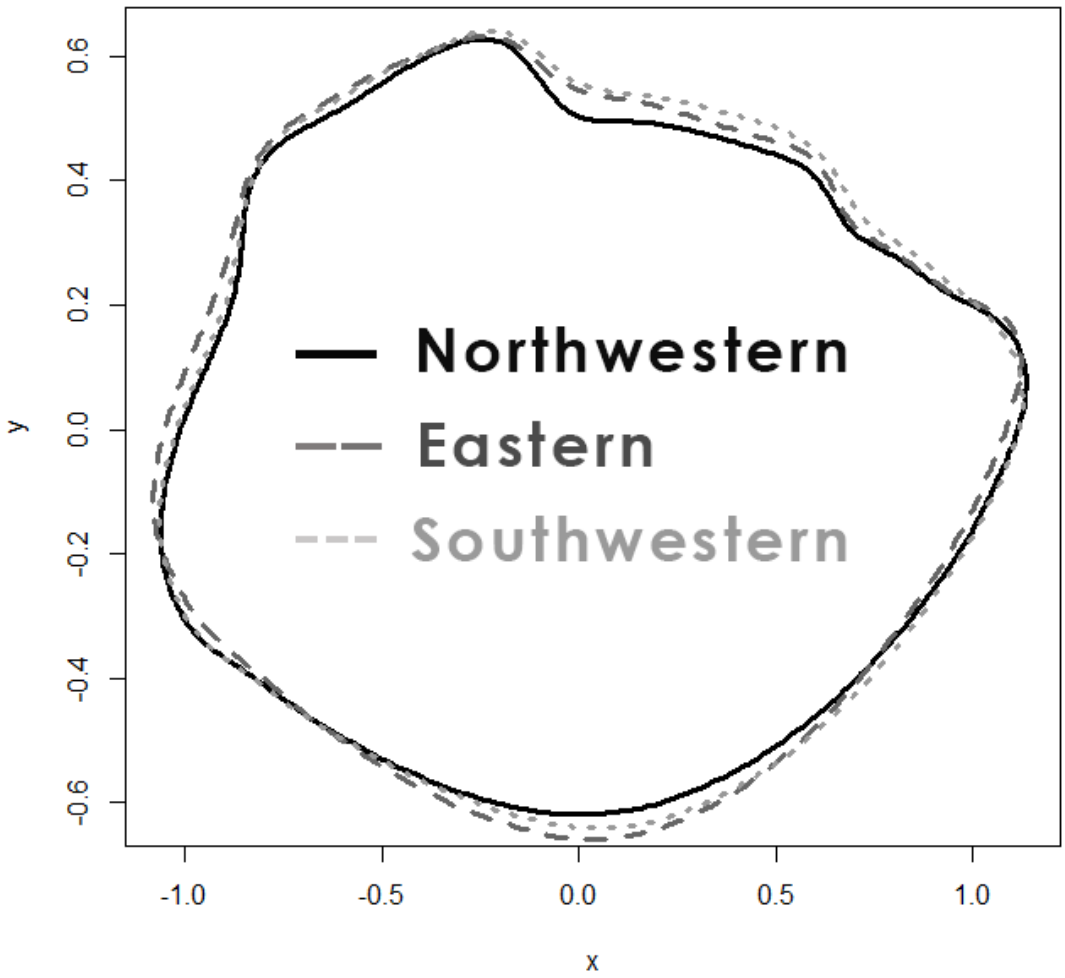

Table 1: Sampling scheme. The number of sampled individuals (Number), their total length (mean and standard deviation) and the sampling years are given by geographical area and year.

Geographical area	Number	Total length (cm) mean±se	Year sampling
Canary Islands	***67***	***19.00±0.93***	***2016***
1: Tenerife Island	67	19.00±0.93	2016
Algeria	***179***	***16.25±3.25***	***2013/2014/ 2015/2016***
2: Gulf of Oran	47	15.50±0.71	2015
3: Gulf of Bejaia	92	15.06±1.70	2013/2014
4: Gulf of Annaba	40	19.12±4.52	2016
Tunisia	***48***	***18.50±1.02***	***2016***
5: Gulf of Tunis	48	18.50±1.02	2016
France	**95**	**19.89±3.75**	**2016**
6: Corsica Island	41	18.50±1.91	2016
7: Gulf of Lions	54	21.00±4.69	2016
Italy	***109***	***18.91±1.91***	***2015***
8: Ligurian Sea	50	19.00±1.74	2015
9: Tyrrhenian Sea	59	18.82±2.07	2015
Greece	***62***	***19.23±2.65***	***2014***
10: Ionian Sea	35	16.80±2.86	2014
11: Aegean Sea	27	20.75±0.71	2014

Table 2: Results of the multivariate mixed-effects model on the shape matrix S. For each explanatory variable, the χ^2 statistic, the associated degrees of freedom (df) and the resulting p-value (P) for a type II test are given. *<0.05; **<0.01, ***<0.001.

Variable	χ^2	df	P
TL	422.599	7	<0.001
SI	34.580	7	<0.001
LO	96.822	7	<0.001
SI:LO	121.923	7	<0.001

Table 3 : Jackknifed correct classification matrix of the Linear Discriminant Analysis for left otoliths (n =560) between the 11 sampling areas based on the residual shape matrix R_{S_L}. The number in each cell represents the number of individuals of the area of origin corresponding to the cell row classified into the predicted area corresponding to the cell column.

		Predicted Area											
		1: Tenerife	2: Oran	3: Bejaia	4: Annaba	5: Tunis	6: Lions	7: Corsica	8: Ligurian	9: Tyrrhenian	10: Ionian	11: Aegean	%correct
Actual area	1: Tenerife	18	4	24	4	8	3	0	1	0	0	5	27%
	2: Oran	0	16	29	1	0	0	0	1	0	0	0	34%
	3: Bejaia	10	8	61	1	2	5	0	4	0	0	1	66%
	4: Annaba	0	5	10	12	3	2	0	8	0	0	0	30%
	5: Tunis	9	0	8	2	22	4	1	1	0	0	1	46%
	6: Lions	3	2	10	2	6	17	4	10	0	0	0	31%
	7: Corsica	1	0	4	3	3	9	12	8	1	0	0	29%
	8: Ligurian	0	0	12	3	3	4	2	22	4	0	0	44%
	9: Tyrrhenian	6	0	12	11	1	5	2	10	12	0	0	20%
	10: Ionian	3	4	4	0	2	1	1	1	0	6	13	17%
	11: Aegean	3	1	3	1	3	0	0	4	0	5	7	26%
	Total	53	40	177	40	53	50	22	70	17	11	27	37%

Table 4 : Jackknifed correct classification matrix of the Linear Discriminant Analysis for right otoliths (n =560) between the 11 sampling areas based on the residual shape matrix R_{S_R}. The number in each cell represents the number of individuals of the area of origin corresponding to the cell row classified into the predicted area corresponding to the cell column.

		Predicted Area											
		1: Tenerife	2: Oran	3: Bejaia	4: Annaba	5: Tunis	6: Lions	7: Corsica	8: Ligurian	9: Tyrrhenian	10: Ionian	11: Aegean	%correct
Actual area	1: Tenerife	31	3	12	2	8	2	6	1	0	1	1	46%
	2: Oran	4	22	20	1	0	0	0	0	0	0	0	47%
	3: Bejaia	7	9	65	1	0	5	1	1	1	2	0	71%
	4: Annaba	2	1	21	6	0	8	0	2	0	0	0	15%
	5: Tunis	6	0	1	1	27	4	3	1	3	0	2	56%
	6: Lions	7	1	2	0	5	25	8	3	2	0	1	46%
	7: Corsica	8	0	1	1	2	12	4	9	3	0	1	10%
	8: Ligurian	1	1	5	1	5	10	8	8	9	1	1	16%
	9: Tyrrhenian	0	0	1	0	2	17	14	11	13	1	0	22%
	10: Ionian	2	1	2	0	3	0	1	2	1	12	11	34%
	11: Aegean	2	0	3	1	4	0	3	3	0	7	4	15%
	Total	70	38	133	14	56	83	48	41	32	24	21	39%

Table 5 : Classification matrix resulting from hierarchical clustering on the residual shape matrix for left otoliths R_{S_L} and right otoliths R_{S_R} ($n = 560$) between the 11 sampling areas. For each area, the cluster gathering the highest number of individuals is highlighted by a shaded cell.

Area	Left otolith			Right otolith			Total
	Cluster 1	Cluster 2	Cluster 3	Cluster 1	Cluster 2	Cluster 3	
1: Tenerife Island	53	14		60	4	3	67
2: Gulf of Oran	36	11		38	1	8	47
3: Gulf of Bejaia	74	18		81	5	6	92
4: Gulf of Annaba	18	22		25	10	5	40
5: Gulf of Tunis	12	36		27	20	1	48
6: Gulf of Lions	26	26	2	25	27	2	54
7: Corsica Island	19	19	3	11	29	1	41
8: Ligurian Sea	35	23	2	28	29	3	60
9: Tyrrhenian Sea	15	32	2	20	28	1	49
10: Ionian Sea	29	6		32	3		35
11: Aegean Sea	17	10		18	9		27
Total	**334**	**217**	**9**	**365**	**165**	**30**	**560**